scientific reports

Check for updates

OPEN

A multi-domain snail metallothionein increases cadmium resistance and fitness in *Caenorhabditis elegans*

Andreas Andric[1], Michael Niederwanger[2], Eva Albertini[1], Pidder Jansen-Dürr[1,4], Stephen R. Stürzenbaum[3], Reinhard Dallinger[2,4]✉, Veronika Pedrini-Martha[2]✉ & Alexander K. H. Weiss[1]✉

Metallothioneins (MTs) are a family of mostly low-molecular weight, cysteine-rich proteins capable of specific metal-ion binding that are involved in metal detoxification and homeostasis, as well as in stress response. In contrast to most other animal species which possess two-domain (bidominial) MTs, some gastropod species have evolved Cd^{2+}-selective multidomain MTs (md-MTs) consisting of several concatenated β3 domains and a single C-terminal β1 domain. Each domain contains three-metal ion clusters and binds three metal ions. The terrestrial snail *Alinda biplicata* possesses, among other MT isoforms, an md-MT with nine β3 domains and a C-terminal β1 domain (termed 10md-MT), capable of binding up to 30 Cd^{2+} ions per protein molecule. In the present study, the *Alinda biplicata 10md-MT* gene and a truncated version consisting of one β3 domain and a single C-terminal β1 domain (*2d-MT*) were introduced into a *Caenorhabditis elegans* knock-out strain lacking a native MT gene (*mtl-1*). The two snail MT constructs consistently increased Cd^{2+} resistance, and partially improved morphological, life history and physiological fitness traits in the nematode model host *Caenorhabditis elegans*. This highlights how the engineering of transgenic *Caenorhabditis elegans* strains expressing snail MTs provides an enhancement of the innate metal detoxification mechanism and in doing so provides a platform for enhanced mechanistic toxicology.

Cadmium (Cd) is one of the most toxic metals to all animal species[1–3]. In humans, Cd induces a variety of pathologies, including, among others, severe disturbances in calcium metabolism, nephrotoxic effects, and proteinuria, as well as anemia[4–7]. An important mechanism that drives the protection against the toxicity of divalent Cd ions (Cd^{2+}) is mediated *via* their complexation by metallothioneins (MTs)[8]. MTs are widespread peptides, found in animals, plants, eukaryotic and prokaryotic micro-organisms, and belong to a heterogeneous protein superfamily consisting of predominantly low-molecular weight, diamagnetic metal-thiolate cluster proteins with the capacity to bind essential and non-essential metal ions with high affinity[9–13]. Although MTs can form complexes with many class-2 metal ions under *in vitro* conditions, *in vivo* most bind predominantly divalent zinc (Zn^{2+}), monovalent copper (Cu^{+}), and divalent cadmium (Cd^{2+})[14]. Metal coordination occurs *via* the sulfur atoms of their numerous cysteine (Cys) residues, which are arranged in repetitive motifs along the peptide chain[15,16]. Typically, the Cys sulfur atoms form metal thiolate clusters with the metal ions, which is instrumental for a solid fold of the three-dimensional protein structure[17–19].

In vertebrates, different MT isoforms are involved in Zn^{2+} homeostasis and metabolism as well as in Cu^{+} regulation[20,21], but also in protection against Cd^{2+} nephrotoxicity[22]. However, MTs have also been reported to protect against a wide range of non-metallic stress factors[23,24]. Mammalian MT2A, in particular, has received considerable attention in recent years due to its pathophysiological role in antioxidant, anti-apoptotic, detoxification and anti-inflammation activity[25–27]. For example, oxidative stress and H_2O_2-induced DNA damage were reduced in MT-competent cells by activation of MT-binding and metal transport systems, whereas MT-deficient cells were more susceptible to Cd^{2+} and reacted to metal exposure primarily through an oxidative stress

[1]Institute for Biomedical Aging Research, University of Innsbruck, Innsbruck, Austria. [2]Department of Zoology, University of Innsbruck, Innsbruck, Austria. [3]Department of Analytical, Environmental and Forensic Sciences, King's College London, London, UK. [4]Center for Molecular Biosciences Innsbruck (CMBI), University of Innsbruck, Innsbruck, Austria. ✉email: reinhard.dallinger@uibk.ac.at; Veronika.Pedrini-Martha@uibk.ac.at; alexander.weiss@uibk.ac.at

response[28]. Due to MTs involvement in diverse species- and cell-specific tasks, their 'true' biological function has been queried and debated[29,30]. According to their presumed role in metal ion regulation, detoxification and stress resistance, most MT genes are readily induced by exposure to Cd^{2+} and other metal ions, as well as by various physiological and toxicological stimuli[31].

The functional human MT genes are located on chromosome 16q13[32]. Their upregulation is mediated by the activity of the metal-responsive/regulatory transcription factor-1 (MTF-1)[33], which involves its binding to metal regulatory elements (MREs) present in multiple copies within the MT promoter[34,35]. In vertebrates, and also most other animal species this multipotent transcriptional regulator of MT genes is evolutionarily highly conserved[36–38], and is involved, apart from metal-dependent upregulation of MT genes, in cellular adaptation to various stress conditions[39–41]. Interestingly, in *Drosophila melanogaster*, it was found that, free metal ion concentrations, but not metals bound to MT, trigger MTF-1 activation, where MTs regulate their own expression through a negative feedback loop[42].

MT primary sequences and structures are much more variable in invertebrates than in mammals and other vertebrates, probably due to the much broader phylogenetic range of invertebrate lineages[30]. An interesting example of this is the MTs of Gastropoda (snails, whelks, limpets and slugs). With some 90,000 known species, they have successfully adapted to the world's most stressful and challenging habitats, which is reflected among other things in the structural diversity of their MTs[43]. Many gastropod lineages have convergently evolved Cadmium-selective MT isoforms, which are mainly responsible for metal-specific tasks such as Cd^{2+} detoxification[43,44]. This detoxification capacity has also been preserved in snail clades that have successfully adapted to new habitats. This is exemplified by the very well-preserved MT structures of the marine periwinkle (*Littorina littorea*) and its close terrestrial relative, *Pomatias elegans*[19,45,46]. The MT gene/protein systems of pulmonate land snails, moreover, have become an invaluable model for studying the metal-selective properties of MTs and their isoform-specific functionality[47–49]. Helicid snails possess three different MT isoforms, two of them with a distinct Cd- or Cu-selective binding capacity, involved in metal-specific functions in favor of their cognate bound metal ions, with CdMT being involved in metal detoxification, and CuMT serving homeostatic Cu regulation[50]. As in vertebrates, the Cd-selective MT genes of snails have several Metal Responsive Elements (MREs) in their promoter regions, which are probably also activated by an MTF-1 or MTF-1-like transcription factor, giving rise to Cd-dependent upregulation upon metal exposure[44,46,51]. Cd^{2+} accumulation occurs primarily in the midgut gland, where the metal is inactivated by CdMTs and stored in lysosomal vesicles, conferring to these animals an increased metal tolerance[1,52,53]. Recently, so-called multi-domain MTs (md-MTs) have been discovered in the terrestrial door snail *Alinda biplicata*[54]. Their upregulation is strongly inducible by Cd^{2+} exposure[54].

The short generation time and invariant developmental lineage have established the nematode *Caenorhabditis elegans* as a model system and transgenic toolbox for controlling the expression and modification of genes with unprecedented resolution[55–57]. Additionally, *C. elegans* serves as a powerful animal model for toxicological studies[30,58]. In response to Cd^{2+} administration, *C. elegans* increases the expression of two MTs (*mtl-1* and *mtl-2*)), and the Cd-specific response gene, *cdr-1*[59]. Whilst *mtl-2* has been hypothesized to be involved in the maintenance of steady state Zn levels, *mtl-1* seems to be linked to the Cd stress response[60]. Unlike all other animal models, however, *C. elegans* does not possess an MTF-1 or MTF-1-like transcription factor[3]. The two *C. elegans* MT peptides, CeMT-1 and CeMT-2, are believed to be key players in the protection against metal toxicity[61–65]. Meanwhile, six *C. elegans* genes that are homologous to the Cd-responsive gene *cdr-1* have been identified and characterized[66]. However, it has been demonstrated that these genes are not required for resistance to metal toxicity[59]. Instead, *C. elegans* relies on the production of phytochelatins (PCs), which play a critical role in the defense against Cd^{2+} toxicity[59,67]. Hence, the lack of Cd^{2+} hypersensitivity in *C. elegans* may be attributed to the compensatory effects of increased PC concentrations when these genes are deleted[59]. It is now suggested that *C. elegans* relies on both MT-mediated and PC-mediated pathways to deal with Cd^{2+} and other metal ions[65]. It has also been demonstrated that depletion of CeMT-1 and CeMT-2 affects all demographic indices measured, resulting in a reduction in worm body size, generation time, brood size and lifespan[3]. Significantly, however, impaired brood size and volumetric growth in MT-deficient *C. elegans* were also observed in the absence of Cd^{2+} exposure[64].

This present study created through CRISPR/Cas9 technology two transgenic *C. elegans* strains in a Cd-sensitive *mtl-1* knock-out background expressing either *10md-MT* (the native 10 domain-MT) or *2d-MT* (the truncated 10md-MT) from the terrestrial snail *Alinda biplicata*. The newly generated transgenics were compared to the *mtl-1* knock-out strain to test their rescue efficiency in terms of life cycle data and mitochondrial oxygen consumption in the presence or absence of Cd^{2+} administration.

Materials and methods

Buffer and media

M9 buffer was prepared according to the Cold Spring Harbor Protocol (doi: https://doi.org/10.1101/pdb.rec081315). *Nematode Growth Medium (NGM)* was prepared according to the Cold Spring Harbor Protocol (doi:https://doi.org/10.1101/pdb.rec081299). *Potassium citrate (1 M, pH 6.0)* was prepared with ddH_2O, using 20 g citric acid monohydrate, and 293.5 g tri-potassium citrate monohydrate per liter, and sterilized by autoclaving. *Trace metals solution* was prepared with ddH_2O, using 1.86 g disodium EDTA, 0.69 g $FeSO_4 \cdot 7\ H_2O$, 0.2 g $MnCl_2 \cdot 4\ H_2O$, 0.29 g $ZnSO_4 \cdot 7\ H_2O$, and 0.025 g $CuSO_4 \cdot 5\ H_2O$ per Liter, and sterilized by autoclaving. *S-medium (basal)* was prepared with ddH_2O, using 5.85 g NaCl, 1 g K_2HPO_4, 6 g KH_2PO_4, and 1 mL cholesterol (5 mg/ml in ethanol) per Liter, and sterilized by autoclaving. *S-medium (complete)* was prepared with ddH_2O, by adding 10 mL 1 M potassium citrate (pH 6), 10 mL trace metals solution, 3 mL 1 M $CaCl_2$, and 3 mL 1 M $MgSO_4$ to 1 L S-medium (basal). All components were added using sterile techniques, and the final buffer must not be autoclaved. *NGM agar plates* were prepared according to the Cold Spring Harbor Protocol (doi: https://doi.org/10.1101/pdb.rec088567). *OP50-1 bacteria* were prepared fresh every week as dense liquid cultures, starting

from a freshly inoculated LB agar plate containing selection antibiotics. *Bleaching solution* was prepared by mixing 500 mM NaOH with 0.8 vol-% NaClO without any further pH adjustments.

Nematode strains

Wild-type (*N2*) nematodes were obtained from the *Caenorhabditis Genetics Center* (CGC, which is funded by NIH Office of Research Infrastructure Programs (P40 OD010440). The *C. elegans* metallothionein CeMT-1 (K11G9.6.1) was deleted, and the resulting *mtl-1(tm1770)* strain backcrossed 6 times[65]. In order to generate the two snail MT knock-in strains, a CRISPR/Cas9 approach was used to add the Alinda biplicata 10md-MT (GenBank: MK648140.1) and 2d-MT (the truncated 10md-MT) in an mtl-1(tm1770) background (SunyBiotech). The 10md-MT protein consists of 9 N-terminal domains (ß3.1-9), whereas the 2d-MT construct consists of only one N-terminal domain (ß3.1) (see Supplementary Figure S1). Both proteins have a C-terminal ß1 domain, and the ß3 sub-structure is connected to the ß1 domain *via* a small linker region. The 2d-MT construct is a bidominial structure and as such, similar to the two native nematode MT isoforms CeMT1 (UniProt: P17511) and CeMT2 (UniProt: P17512). Both *C. elegans* MTs have, however, a few additional amino acids after the last cysteine in their C-terminal region. Both constructs were re-introduced into the genomic region where the *mtl-1* was removed. Hence, the respective construct is positioned downstream of the *mtl-1* promoter. The resulting strains PHX3856 *mtl-1* (syb3856) and PHX3852 *mtl-1*(syb3852) (to be obtained on request from SunyBiotech) were verified by sequencing using genotyping primers: [*AGT GCA CAA ATG AAG GCT GCA A*] (forward), and [*GGC AGA TAC AAG TAA TAT ACA CAT T*] (reverse). PHX and syb are the strain designation and allele designation, respectively, and both PHX and syb were confirmed by the WormBase (https://wormbase.org).

mRNA isolation, reverse transcription and qRT-PCR

To verify the gene expression of the 10md-MT and 2d-MT constructs in the respective strains, qRT-PCR was performed. Therefore, nematode pellets were frozen in liquid nitrogen and homogenized with glass beads (Precellys, Bertin Instruments, Montigny-le-Bretonneux, France). Total RNA was isolated using the RNeasy®Plant Mini Kit (QIAGEN, Venlo, The Netherlands) with on-column Dnase 1 digestion (QIAGEN, Venlo, The Netherlands). RNA integrity was visually checked on a 1.5% agarose gel (Biozym, Germany) and quantified using the NanoDrop™ 2000 (Thermo Fisher Scientific, Waltham, MA, USA). First-strand cDNA was synthesized from 450 ng total RNA using the AccuScript High-Fidelity Reverse Transcriptase Synthesis Kit (Agilent Technologies Inc., Santa Clara, California, USA) in a 20 µL reaction for subsequent real-time detection PCR. To confirm the gene expression of the 10md-MT and 2d-MT construct in the respective nematode strain, primers and setup were applied as described elsewhere[54]. Briefly, qRT-PCR of cDNAs was performed with Power SYBR Green (Applied Biosystems, Thermo Fisher Scientific, Waltham, MA, USA) on a QuantStudio 3 (Applied Biosystems, Thermo Fisher Scientific, Waltham, MA, USA). The following PCR protocol was used for 40 cycles: denaturation at 95 °C for 15 s, annealing and extension combined at 60 °C for 60 s. The 10 µL PCR reaction contained 1 µL cDNA, 5 µL Power SYBR Green PCR Master Mix, 1 µL U-BSA (Merck, Darmstadt, Germany), 1 µL water (Direct Q®3 UV, Merck Millipore SAS, Molsheim, France), and 1 µL of each forward and reverse primer. To exclude false positive signals by genomic DNA, no-RTs were generated and measured. The primer sequences used were: Forward: 5`-GTGGTGATGGCTGCACATGT-3`, Reverse: 5`-CGCTGGGCCTGTACACTCTT-3`.

Cadmium exposure

Wild-type nematodes were raised in liquid culture to assess the actual amount of Cd^{2+} taken up by the worms under given experimental conditions. Following the guidelines outlined in the *WormBook* (www.wormbook.org, *5. Growth of C. elegans in liquid medium*), nematodes were raised in 50 mL S-medium (complete) at nominal concentrations of 0 µg/g (0 µM), 0.3 µg/g (2.5 µM), and 1.3 µg/g (12 µM) Cd^{2+}, and subsequently harvested by centrifugation at low gravity (300 x g; 1 min). The resulting cloudy supernatant, still including almost all OP50-1 bacteria, was carefully decanted from the nematode pellet. The pellet was then washed once with fresh 1 mL of S-medium (complete), and the wash solution was combined with the previously collected supernatant to prevent bacterial loss. Subsequently, the bacteria were separated from the liquid *via* centrifugation at *10.000 x g* for 10 min, and the supernatant was carefully discarded. Cd^{2+} content in all samples was assessed using atomic absorption spectrophotometry.

Synchronization of nematodes

An NGM agar plate with a mixed worm population was chunked and nematodes were cultivated for 3–4 days at 20 °C. To obtain synchronized nematodes in the *L1* larval stage, 30 adult worms were transferred to NGM agar plates. Fresh *Bleaching solution* was used to fully dissolve the worms. Remaining eggs were washed off the plates with 5 mL *S-medium (complete)* and collected in a 15 mL tube, shaken overnight on an orbital shaker. The following day, *L1* larval stage worms were obtained *via* centrifugation at low gravity (300 *x* g, 2 min), washed three times using 5 mL of ddH_2O, and then washed two times using 5 mL *S-medium (complete)*. After each wash, *L1* larval stage worms were obtained *via* centrifugation at low gravity (300 *x* g, 2 min). The nematodes were eventually transferred onto NGM-plates spotted with OP50-1 bacteria and incubated at 20 °C for 72 h to reach adulthood (L4 stage / young adult).

Nematode morphology assessment

Nematodes were synchronized and transferred onto NGM plates spotted with OP50-1 bacteria. For each worm, a fresh droplet of 10% NaN_3 solution (about 2–5 µL) was placed on an NGM agar plate, and the worm was transferred into the droplet. The length and diameter of the worms were analysed using a ZEISS *Discovery. V12 SteREO* microscope with JENOPTIK camera *ProgRes CT3 USB* at 9.0 µm resolution. Measurements were taken by determining the size in pixels with the evaluation software JENOPTIK *ProgRes ® CapturePro 2.8.8*. The

length and diameter of each worm from each strain were normalized to the average length of assessed wild-type worms. The diameter of the worms was recorded as the greatest body diameter. The body mass of the nematodes was calculated using the Andrássy formula[68] $W = (L * D^2)/(1.6*10^6)$, where W represents the mass (in µg) per individual, L is the nematode length (in µm) and D is the greatest body diameter (in µm).

Egg laying assay

Starting with a working plate of (un)synchronized worms, single young adult worms were transferred onto fresh NGM agar plates (10 cm) spotted with OP50-1 bacteria (see Supplementary Figure S2A). This is defined as *day 0 of the egg-laying assay*. After the worms had laid their eggs, single eggs were transferred to individual fresh NGM agar plates (6 cm) spotted with OP50-1 bacteria, where new worms were expected to hatch within two days. At this stage of the assay, the *hatching rate* of the individual strain was determined by calculating the fraction of hatched worms divided by the number of eggs previously transferred. It is important to note that although no Cd^{2+} has been applied yet, however, the presence of minor traces of bivalent metal ions (Ca^{2+}, Mg^{2+}, Cd^{2+}, Zn^{2+}) in the Millipore grade water used (in this case based on Austrian water quality) could not be excluded. Hatched worms were then transferred onto fresh NGM agar plates (6 cm) spotted with OP50-1 bacteria and containing three different nominal concentrations of Cd^{2+}: 0 µM, 2.5 µM, and 12 µM. This is defined as *day 1 of the egg-laying assay*. Over a period of 5 days (see Supplementary Figure S2B), each day the adult nematode on the plate was transferred onto a fresh NGM agar plate (6 cm) spotted with OP50-1 bacteria and the same Cd^{2+} concentration, respectively. At this stage of the assay, the *death rate* of the individual strain was determined by calculating the fraction of worms that died during the assay divided by the number of worms previously transferred. If a worm died during the assay, all data obtained from that worm were excluded from the final data pool to ensure that the combined egg-laying data referred only to worms that survived for the whole period of 5 days. The *viable offspring* resulting from laid eggs at the individual days was determined by counting L2 stage larvae 2 days after the worm transfer. The viable offspring per adult worm was then associated with the day of worm transfer (dating two days back in time, starting from day 0).

Seahorse flux analysis with intact nematodes

The Seahorse extracellular flux analyzer has become a versatile tool to measure rates of oxygen consumption and extracellular acidification in adhesive cells and cells in suspension (see also the supplementary material provided with this manuscript). Several protocols have recently been developed to apply this technique to intact nematodes[69–71]. Among other applications, such as targeting mitochondrial dynamics and homeostasis processes[72,73], this technique also allows for assessing the effects of toxins and other agents on the respiration of viable and intact nematodes[70,74], instead of respirometry studies on isolated mitochondria. Inspired by these protocols, in the present study, Seahorse Flux Analysis was applied to nematodes of the different strains using the Agilent Seahorse HS mini analyzer. One day prior to the experiment, the Seahorse cartridge was rehydrated according to the vendor's defined protocol and put at 37 °C without CO_2. In this study, young adult wild-type nematodes were tested against another strain of interest in technical triplicates on a default 8-well Seahorse cartridge. Synchronized young adult nematodes were collected by gentle washing three times with a total of 7 mL of autoclaved M9 buffer, using a 25 mL serological pipette, to avoid stressing the nematodes through friction or force. For better washing results, nematodes were then centrifuged in a 15 mL FALCON tube (300 x g for 2 min). The top 5 mL of the formed supernatant was carefully discarded using a 1 mL pipette. The nematode pellet was resuspended by adding 5 mL of fresh M9 buffer (a total 7 mL). This washing procedure was performed three times in total. The top 6 mL of the formed supernatant was carefully discarded using a 1 mL pipette. The top of a 1 mL plastic tip was cut off to obtain a wider hole. Using this tip, 500 µL of a 0.1% Triton-X solution in S-medium (complete) was pipetted up and down to coat the interior of the tip. This procedure prevents nematodes from sticking to the plastic. Worms were then gently pipetted onto the center of an unspotted NGM plate. A glass Drigalski spatula was used to gently distribute the nematodes over the whole plate, leaving a small gap towards the rim. At this point, one needs to wait until all liquid has dried out, and the last described step helps to speed up the process without stressing the worms. At least one hour before measurement, the rehydrated Seahorse cartridge was equilibrated with calibrant solution. A Seahorse cell-culture plate was prepared by filling each well with 200 µL of S-medium (complete). The Seahorse cartridge was filled with assay chemicals (according to the SOP), and during the Seahorse equilibration step, selected young adult worms were picked from the dried NGM plate, and put into the respective wells of the Seahorse plate (~ 30 worms per well). The actual number of nematodes in each well was determined using a microscope right after the Seahorse experiment. All data were then normalized to these numbers.

Atomic absorption spectroscopy (AAS)

The extracted nematode pellets and bacteria pellets were oven-dried at 68 °C and digested under pressure in 2 mL flat-bottom tubes (Eppendorf, Hamburg, Germany) with a 1:1 mixture of nitric acid (65%) (Suprapure, Merck, Darmstadt, Germany) and deionized water in an aluminum oven with a heated lid at 68 °C. After complete digestion, the samples were diluted to 2 mL with deionized water. The supernatant S-buffer was measured alongside the nematode and bacteria samples. Metal concentrations were measured through a graphite furnace using an atomic absorption spectrophotometer (model Z-8200, Hitachi, Tokyo, Japan). The system was calibrated using *Titrisol metal standard solutions* (Merck, Darmstadt, Germany) containing 1% nitric acid. Certified standard reference material from the National Research Council in Canada was used to determine the accuracy of metal measurements (*TORT-2 Lobster Hepatopancreas* Reference Material for Trace Metals; National Research Council Canada) ($n = 5$).

Statistics, graphs, and terminology

Statistical comparisons of strain data were performed using GraphPad Prism (version 5, Windows). For each comparison, a two-tailed Welch's t-test was used to compare the means of two independent groups when the assumption of equal variances was violated, allowing for different variances between the two groups being compared. Prior to this analysis, four types of normality tests were applied to ensure a normal distribution of data points (D'Agostino-Pearson, Shapiro-Wilk, Anderson-Darling and Kolmogorov-Smirnov; all provided in the GraphPad Prism software). Graphs in all figures were obtained by GraphPad Prism. Stars in all diagrams represent p-values as follows: * $p \leq 0.05$, ** $p \leq 0.01$ and *** $p \leq 0.001$. The terms "nearly significant" and "near to significance" refer to p-values of $p < 0.07$, to describe an observed effect that reflects a biological trend. To describe the rescue effects, following terms are used: partial rescue: The snail-MT strain performs better than *mtl-1*, but not as well as the wild-type. Complete rescue: the experimental strains perform the same as the wild-type strain. Outperformance: The snail-MT strains perform better than *mtl-1* and wild-type worms.

Results

Strain preparation and verification

Strain preparation and verification methods are described in detail in the Materials and Methods section. The expression of 10md-MT and 2d-MT in *C. elegans* knock-in strains was confirmed by quantitative PCR analysis (qRT-PCR) (see Supplementary Figure S3).

Cd^{2+} uptake in liquid culture and on NGM agar plates

As illustrated in Fig. 1, the measured Cd^{2+} concentrations in the S-medium closely matched the nominal exposure concentrations of 0, 0.3 and 1.3 mg/L (µg/g wet weight), corresponding to 0 µM, 2.5 µM and 12 µM Cd^{2+}, respectively. Concurrently, the metal concentrations increased proportionally within the nematodes and the bacteria, with higher concentrations observed in the latter compared to nematode worms. It is therefore suggested that Cd^{2+} is incorporated into nematodes *via* their food source, represented by the OP50-1 bacteria,

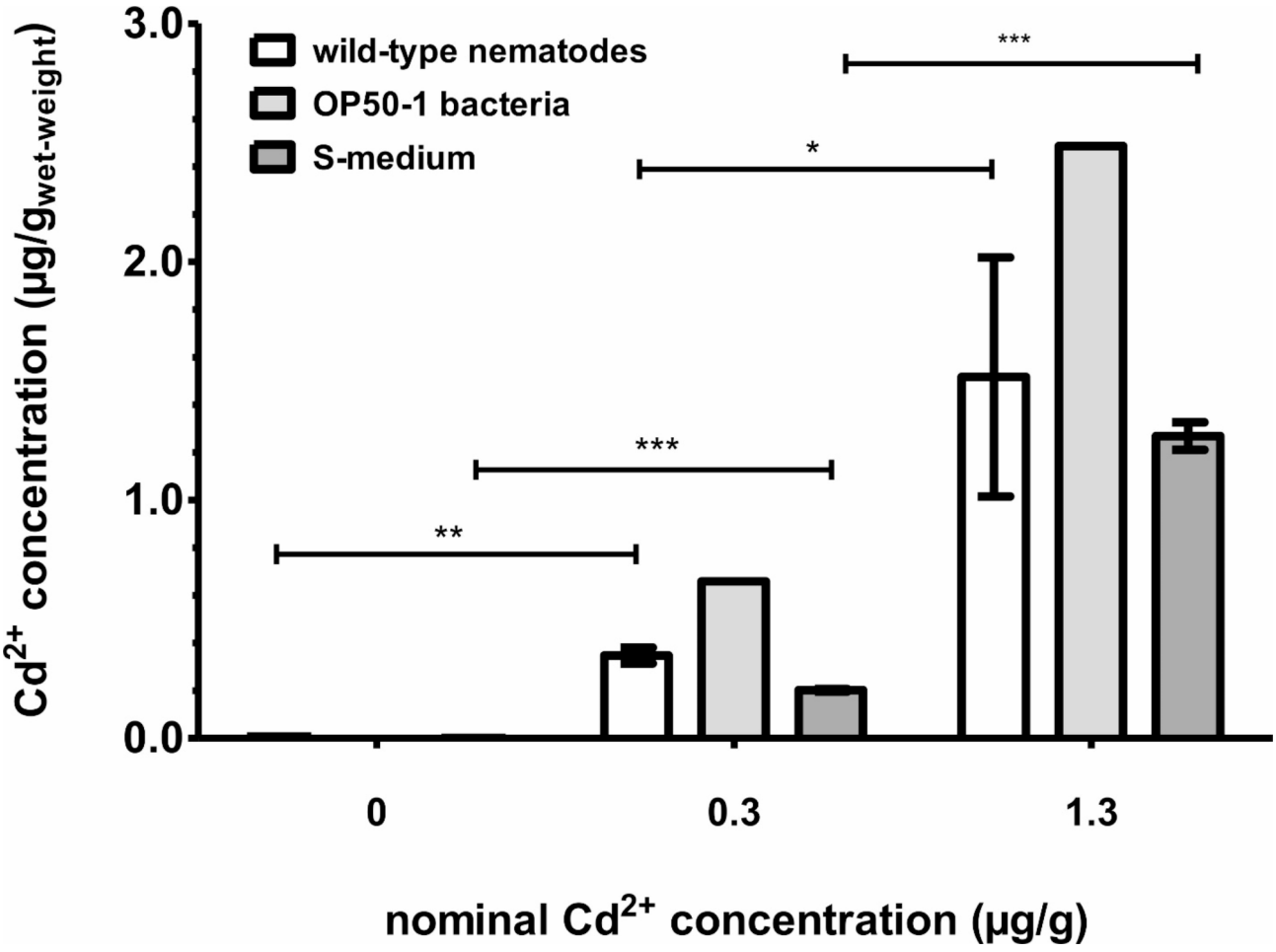

Fig. 1. Cd^{2+} uptake by nematodes in liquid culture. *N2* nematodes were raised in 50 mL of liquid culture containing Cd^{2+} at concentrations of 0 µg/g (0 µM), 0.3 µg/g (2.5 µM), and 1.3 µg/g (12.0 µM). After separation *via* centrifugation and washing steps, Cd^{2+} concentrations were measured *via* AAS separately in nematodes, bacteria (OP50-1), and supernatant (S-buffer). Significance is marked by asterisks.

which in turn acquire the metal from the medium and are subsequently incorporated into the nematodes' gut-region (Fig. 1). Although these metal uptake experiments were performed for the wild-type strain only, it is assumed that the uptake data and corresponding Cd^{2+} concentrations would exhibit similar trends for worms of the other strains as well. Cd^{2+} concentrations in bacteria were analyzed only once, while nematodes and S-medium supernatant were measured in technical triplicates. In all experiments where nematodes were cultivated on NGM agar plates, Cd^{2+} was applied to OP50-1 cultures, which were then used for spotting. Additionally, we investigated uptake using NGM agar plates cast with defined Cd^{2+} concentrations in the agar, while using OP50-1 bacteria that had not been previously contaminated with Cd^{2+} before spotting. In these control experiments, no Cd^{2+} uptake by the worms was observed (data not shown), further confirming that the primary source for Cd^{2+} incorporation into nematodes is their bacterial food source. This study was primarily focused on the functional consequences of MT expression in terms of biological outcomes such as growth, mitochondrial function, and overall resilience to cadmium stress. Furthermore, cadmium uptake alone does not necessarily reflect the functional detoxification capacity of the protein, which we believed could be better assessed through our life cycle and mitochondrial respiration assays. Nevertheless, we acknowledge the merit of this approach and plan to include cadmium uptake studies in future experiments.

Nematode size and mass

The average nematode body length, maximum diameter and body mass of all strains are presented in Fig. 2 (with 10 worms per strain). It was observed that the worms of the *mtl-1* and *2d-MT* strains had shorter body lengths compared to the wild-type worms (Fig. 2A). In contrast, the *10md-MT* strain revealed no difference in body size compared to the wild-type strain and the *mtl-1* strain. This rescue effect is therefore considered to be partial, as the wild-type worms show a clear difference in body size compared to the *mtl-1* knockout strain. In contrast, worms of the *10md-MT* strain were significantly smaller in diameter compared to the wild-type strain, whereas in this case the *2d-MT* strain not only increased markedly in body diameter compared to the *mtl-1* and *10md-MT* strains, but also outperformed the wild-type worms (Fig. 2B). Consequently, the average body mass of the *2d-MT* strain was comparable to the wild-type reference strain (Fig. 2C). In particular, the body mass of the *10md-MT* and *mtl-1* worms was significantly smaller compared to wild-type control worms, whereas the 2d-MT knock-in appeared to rescue this effect (Fig. 2C). Overall, the *mtl-1* worms displayed a generally weaker and seemingly almost frail phenotype. This was particularly evident in their maximum diameter of *mtl-1* worms compared to all other strains (Fig. 2B). To visually verify these data, worms were picked from an NGM plate, sedated, and examined under the microscope to observe any changes in their morphology and egg laying behaviour. Overall, the morphology of worms from the knock-in strains (*10md-MT* and *2d-MT*) appeared to be more robust than that of the *mtl-1* worms, and almost resembled the appearance of wild-type worms (see Supplementary Figure S4), as evidenced by the quantitative data above. The truncated MT form was selected based on studies that suggested this specific truncation might affect the protein's structure and function in a way that could influence its binding capacity. The main reason for this suggestion is the fact that the two-domain structure of the truncated form resembles very much the two-domain CdMTs found in many other snails of the lineage of *Stylommatophora* (to which *Alinda biplicata* belongs). It also resembles in its size and its structure the native MTs of *Caenorhabditis elegans* much more so than the md-MT of *Alinda biplicata*. The use of the truncated form should therefore allow a direct comparison between the functional performance of 'normal' two-domain invertebrate MTs and the natural multidomain MT aberrations evolved in a range of snails from different lineages. In this way, we could directly assess whether a loss of certain functional domains (compared to the full-length 10md-MT) could alter cadmium-binding efficiency and subsequent detoxification processes. Regarding the differences in worm size, we speculate that the truncated form might influence growth through a cadmium-independent mechanism, possibly due to altered interactions with other cellular pathways or stress-response mechanisms. However, more research will be needed to fully elucidate this effect.

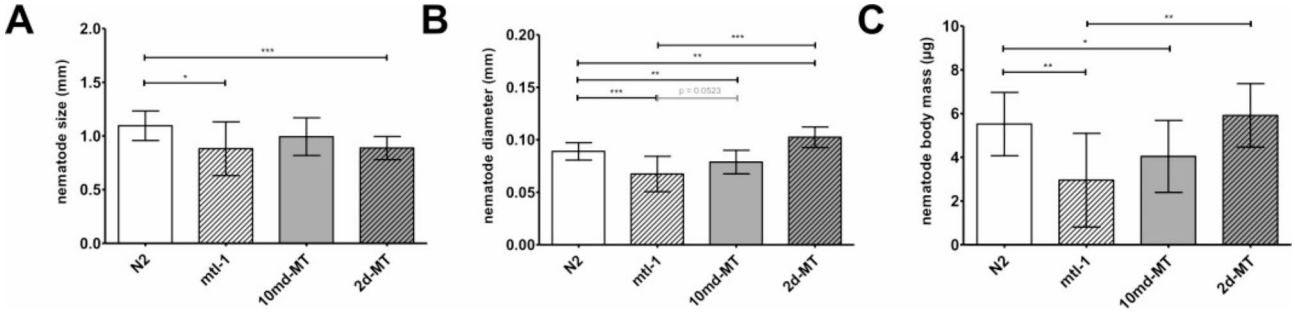

Fig. 2. Nematode strain characterization. Average worm length (**A**), diameter (**B**) and body mass (**C**) were determined for the wild-type strain (*N2*), the mtl1 knockout strain (*mtl-1*) and the two snail MT knock-in strains carrying the full 10md-MT (*10md-MT*) and the 2d-MT construct (*2d-MT*) of Alinda biplicata under 0 µM Cd^{2+} conditions. Statistical analysis was performed on 15 worms per strain. Error bars represent the standard deviation at 95% confidence. Gray bars denote non-significant (ns) differences, or close-to-significant differences ($p < 0.08$) where a p value is given. A p-value close to significance (added in the figure above respective bars) indicates a biological trend. Significance is marked by asterisks.

While the main function of MTs is detoxification and homeostatic regulation of metals as well as stress adaptation, *C. elegans mtl-1* and *mtl-2* have been shown to also play a certain role in regulating the worm's growth and fertility[59,75]. Hence, the frail appearance of *mtl-1* knockout worms probably indicates that these worms might lack the ability to retain their eggs under stress conditions, and their low body mass may also be linked to complications in maintaining a functional egg facility system, resulting in severe differences compared to the other strains.

Egg laying assay

The data derived from the egg-laying assay include the proportion of worms successfully hatched from the different strains, the Cd^{2+}-dependent mortality of the strains during hatching, and the proportion of viable offspring in the different strains at increasing Cd^{2+} concentrations. Figure 3A shows the percentage of successfully hatched worms of the different strains under control conditions. Compared to the wild-type strain, worms of the *mtl-1* strain, and both (md)MT strains hatched at a comparable rate at a nominal exposure concentration of 0 µM Cd^{2+}. Interestingly, worms of the *10md-MT* strain exhibited a significantly higher hatching rate compared to the *mtl-1* strain, but not relative to the wild-type (Fig. 3A). Although the details of this observation remain unclear, it suggests that the 10md-MT knock-in confers a more robust phenotype to the worms, possibly indicating a beneficial role of the 10md-MT gene in the reproductive fitness of *C. elegans*. This is confirmed by the observed mortality during the five days of exposure to elevated Cd^{2+} concentrations (0, 2.5 and 12 µM) (Fig. 3B). Overall, the mortality of worms in all strains increased with rising Cd^{2+}-concentrations in a dose-dependent manner with the wild-type and MT strains (and to a lesser extent the *mtl-1* strain). Worms from *2d-MT* strain exhibited a significant trend towards a lower mortality compared to worms from the wild-type and *mtl-1* strains (Fig. 3B). This trend was nearly significant ($p < 0.07$) for worms from the *10md-MT* strain. This suggests that in *C. elegans*, the Cd^{2+} detoxification capacity of the expressed snail 10md-MT and its truncated 2d-MT variant outperforms the metal detoxification function of the own native CeMT1 protein. This may be explained by the fact that in *C. elegans*, the CeMT1 protein is less selective for Cd^{2+} binding[76], compared to the highly Cd^{2+}-selective md-MTs of *Alinda biplicata*[54]. Furthermore, the 10md-MT of *Alinda biplicata* can bind up to 30 Cd^{2+} ions per protein molecule, compared to only 7 divalent metal equivalents bound by the native *C. elegans* CeMT1 protein[76]. In the present data, the mortality of *mtl-1* worms appears to be like their wild-type counterparts (Fig. 3B). However, this is somewhat biased because a considerable part of the egg-laying study was spent collecting sufficient eggs for the biological replicate data from the *mtl-1* worms. The hatching worms from the few healthy eggs that were obtained from this strain, however, had a similar mortality rate than the wild-type worms. Of note, we did not observe any bagging effects (eggs hatching within the parental worm), a phenomenon that was described in some other studies[77]. Finally, the visual egg morphology was comparable between worms of all strains (see Supplementary Figure S5).

Data from the egg-laying assay referring to the viable offspring of adult nematodes from all strains and for all nominal Cd^{2+}concentrations applied (0 µM, 2.5 µM, 12 µM) are presented in Fig. 4. The number of viable offspring of the wild-type strain declined in a concentration-responsive manner (Fig. 4A), replicating the data of previous studies[64,65]. Knocking out the native MT gene in the *mtl-1* strain[64,65] decreased the performance

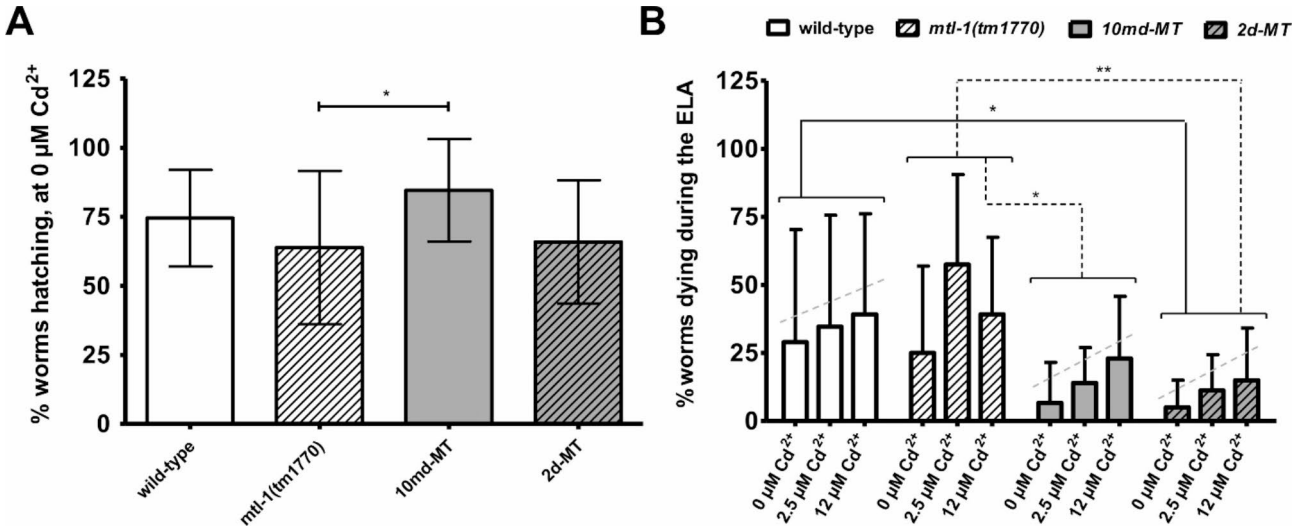

Fig. 3. Nematode hatching rate and mortality during the setup phase of the Egg-laying assay. Diagrams display the hatching rate at 0 µM Cd^{2+} conditions (**A**), and death rates (**B**) for the strains *N2*, *mtl-1*, *10md-MT*, and *2d-MT* under an exposure regime of rising Cd^{2+} concentrations (0, 2.5 and 12 µM Cd^{2+}). at. Statistical analysis was conducted on the following sample size: *N2*: 16 worms in 5 experiments; *mtl-1*: 11 worms in 8 experiments; *10md-MT*: 19 worms in 5 experiments, *2d-MT*: 21 worms in 5 experiments. Error bars indicate the standard deviation at 95% confidence. Welch's t-tests have been performed on data groups pooled among Cd^{2+} concentrations, as indicated by the horizontal brackets. Significance is marked by asterisks.

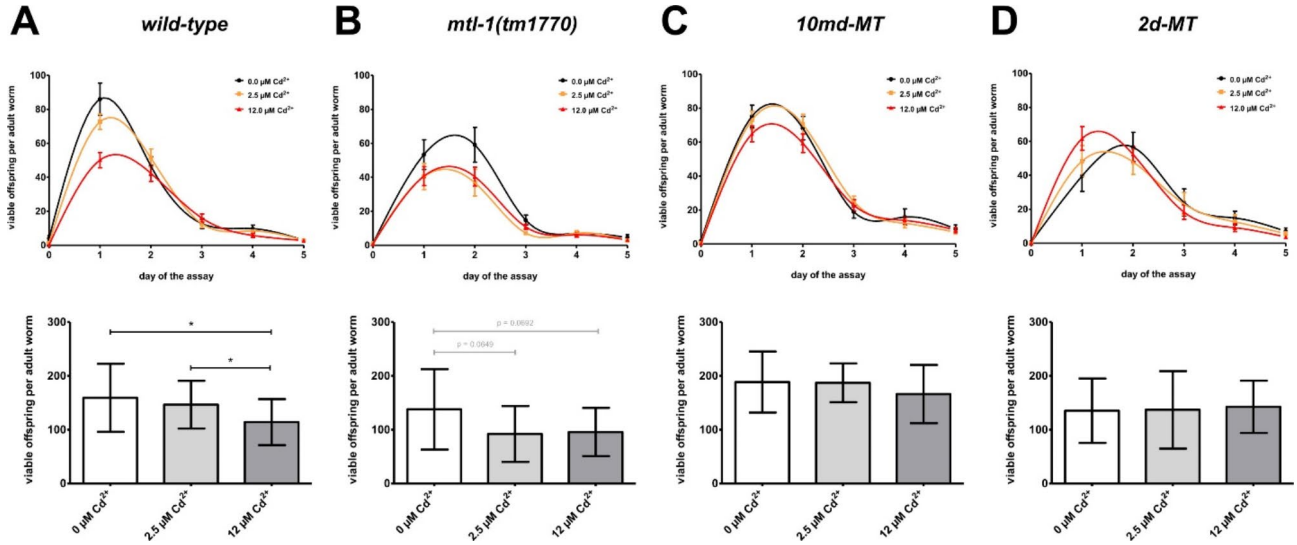

Fig. 4. Egg-laying assay. The top diagrams display the viable offspring (ordinate) counted for the given day (abscissa) (**A–D**). The overall number of viable offspring (area under the curve) is presented in the column diagram below (**E–G**). Data for the four strains *N2* (**A**), *mtl-1* (**B**), *10md-MT* (**C**) and *2d-MT* (**D**) are shown. These data are further characterized by different concentrations of Cd^{2+}: (**E**) 0 µM Cd^{2+}, (**F**) 2.5 µM Cd^{2+}, and (**G**) 12 µM Cd^{2+}. Statistical analysis included technical replicates: *N2*: 5 experiments; *mtl-1*: 8 experiments; *10md-MT*: 5 experiments; 0 µM: *N2*: 16 worms, *mtl-1*: 11 worms; *10md-MT*: 19 worms; *2d-MT*; 13 worms; 2.5 µM: *N2*: 16 worms; *mtl-1*: 9 worms; *10md-MT*: 23 worms; *2d-MT*; 15 worms; 12 µM: *N2*: 18 worms; *mtl-1*: 12 worms; *10md-MT*: 20 worms; *2d-MT*; 18 worms. Error bars indicate the standard error at 95% confidence. Significance is marked by asterisks.

of these worms under Cd^{2+} exposure (Fig. 4B, and F). Data for the *10md-MT* strain resembled a rescue effect for viable offspring at all nominal Cd^{2+} concentrations applied, suggesting that the 10md-MT gene of *Alinda biplicata* confers robust Cd resistance to the nematode model under the present experimental conditions (Fig. 4C). A rescue effect in terms of viable offspring was also apparent for the truncated *Alinda biplicata* MT gene construct expressed in the *2d-MT* strain (Fig. 4D). A direct comparison between strains shows that these effects are apparently a function of the Cd^{2+} concentrations applied (Fig. 4E–G). Interestingly, the rescue effect in worms of the *10md-MT* strain under Cd^{2+} stress was pronounced and even outperformed the Cd^{2+} resistance of the wild-type strain (Fig. 4F and G). Not shown in these data, but observed in the laboratory, the nematodes of the *10md-MT* strain appeared to be more vivid and generally healthy-looking when observed on the plates, whereas worms of the other strains where visibly stressed. A trend towards outperformance ($p \leq 0.07$) was also observed at the highest concentration of Cd^{2+} (12.0 µM) in the offspring of *2d-MT* worms, nearly equal to that observed in *10md-MT* individuals (Fig. 4G).

The functionality of the *C. elegans* reproductive system depends on several anatomical and physiological features, including the egg-laying apparatus[78], as well as the mode of energy allocation for reproduction[79]. In this perspective, it is highly interesting that the native *C. elegans* MTs, CeMT1 and CeMT2, are not only involved in protection against Cd^{2+}- induced stress during reproduction, but also play a critical role in reproductive performance, growth, and development in the absence of Cd^{2+} exposure[80,81].

It is therefore reasonable to assume that the snail 10md-MT and 2d-MT proteins may also contribute, apart from Cd^{2+} detoxification, to an improved reproductive performance in *C. elegans*, as suggested at least in the *10md-MT* strain (see Fig. 3A). This is remarkable, considering that, in *Alinda biplicata*, the *10md-MT* gene and its expressed protein are specifically involved in Cd^{2+} detoxification, with little evidence suggestive of an alternative functionality[54]. A possible explanation is that MTs exert their functional specificity under the control of the cellular system in which they are expressed[49], so that transgenic MTs or MT constructs expressed in a non-native system may take on some functional tasks imposed on them by the host cells, in addition to their original specificity.

Oxygen consumption rates determined with seahorse flux analysis

Cd^{2+} has the potential to induce oxidative stress at the cellular level, leading to adverse effects on cellular functions, in particular affecting enzyme activity and reducing the efficiency of cellular respiration[82]. This reduction in efficiency can result in decreased energy production, compromised cell viability, and disruption of normal cellular functions. In particular, the effect of Cd^{2+} on cellular respiration is manifested by its direct targeting of mitochondria, disrupting their structure and function, and impairing the activity of the electron transport chain[83]. In addition, Cd^{2+} directly inhibits enzymes in the electron transport chain, such as complex III and complex IV, leading to a disruption in the flow of electrons and a compromise in the efficiency of cellular respiration[84]. This leads to reduced production of ATP, the primary energy currency of the cell. The change

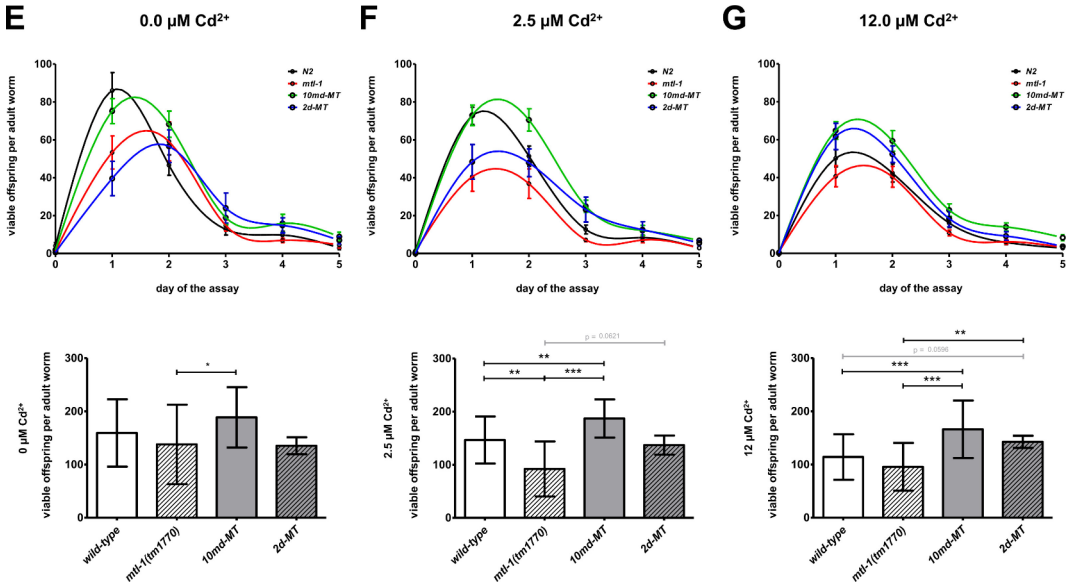

Figure 4. (continued)

in oxygen consumption rates upon uncoupling oxidative phosphorylation from ATP synthesis (cellular spare capacity) is a proxy for studying oxidative stress in nematodes[70].

In the present work, oxygen consumption rates were determined in intact worms (*N2*, *mtl-1(tm1770)*, *10md-MT* and *2d-MT*) as a function of Cd^{2+} exposure, using Seahorse Flux Analysis (Fig. 5) by measuring respiration under routine conditions, followed by respiration after uncoupling with FCCP for calculation of spare capacity, and terminated by stopping respiration by addition of NaN_3. Two sets of respiration curves in technical triplicates are reported in Fig. 5A, showing the respiratory performance of worms of each strain without Cd^{2+} exposure (0 µM Cd^{2+}) (Fig. 5A, left panel), and under high Cd^{2+} exposure conditions (12 µM Cd^{2+}) (Fig. 5A, right panel). Both curves show a significantly reduced spare capacity of *mtl-1* worms compared to wild-type nematodes without and at high Cd^{2+} exposure conditions (Fig. 5B), suggesting that the already fragile *mtl-1* worms are more stressed in the presence of Cd^{2+}. On the contrary, the surplus capacity of *10md-MT* worms saw a complete and statistically significant recovery to the levels seen in control worms (Fig. 5A and B), with a slight further enhancement noted in the presence of Cd^{2+}.

Cd^{2+} stress disrupts cellular respiration in nematodes by impacting mitochondrial function, disturbing the electron transport chain, and triggering oxidative stress[84]. This is not reflected by differences in oxygen consumption rates when comparing worms of the different strains under Cd^{2+} exposure versus Cd^{2+}-free conditions. However, the present data show a significantly reduced spare capacity for the MT-deficient *mtl-1* strain compared to the wild-type worms even under control conditions. This effect is exacerbated under Cd^{2+} exposure (Fig. 5) but is rescued by both snail MT knock-in strains (*10md-MT* and *2d-MT*) up to the respiratory levels seen in the wild-type strain.

Synopsis: snail *multi-domain MT genes* elicit multiple rescue effects in *mtl-1* deficient *C. elegans* strains

Taken together, the present data clearly show that the *10md-MT* gene and its truncated variant *2d-MT* from the terrestrial snail *Alinda biplicata* induce rescue effects in *C. elegans* who's native *mtl-1* gene activity has been knocked out. While nematodes of the *mtl-1* strain appear to be generally less viable and show increased sensitivity to Cd^{2+} exposure, worms of the *10md-MT* and *2d-MT* strains show improved life history traits in terms of reproductivity, survival, and respiratory energy metabolism, in addition to a conferred higher resistance to Cd^{2+} exposure. In all assays conducted in this study, worms of both snail MT strains at least matched the performance of the *mtl-1* strain and the *md-MT* knock-in even outperformed wild-type nematodes in some life history traits (see Fig. 6).

Conclusion and outlook

Caenorhabditis elegans is a powerful animal model for toxicological studies[30,58,70]. This also applies to studies with toxic metals, where the nematode's own metallothionein CeMT-1 and CeMT-2, protect the worms from metal toxicity[61–65]. Their deletion leads to a reduction in the body size, the generation time, the brood size, and the lifespan[3], in some cases even in the absence of Cd^{2+} exposure[64]. The present study shows that a CRISPR/Cas9-mediated replacement of CeMT-1 (*mtl-1*) by the *10md-MT* gene from the snail *Alinda biplicata* and a truncated variant (*2d-MT*) creates viable nematode strains that are able to rescue, even outperform, traits, including the level of mitochondrial respiration. It also appears that the two rescue strains may behave differently in restoring important metabolic functions. The present data extends previous work[64] by providing further evidence that the biological role of MTs in *C. elegans* is not limited to Cd^{2+} detoxification. Notably, *C. elegans* also produces PCs in

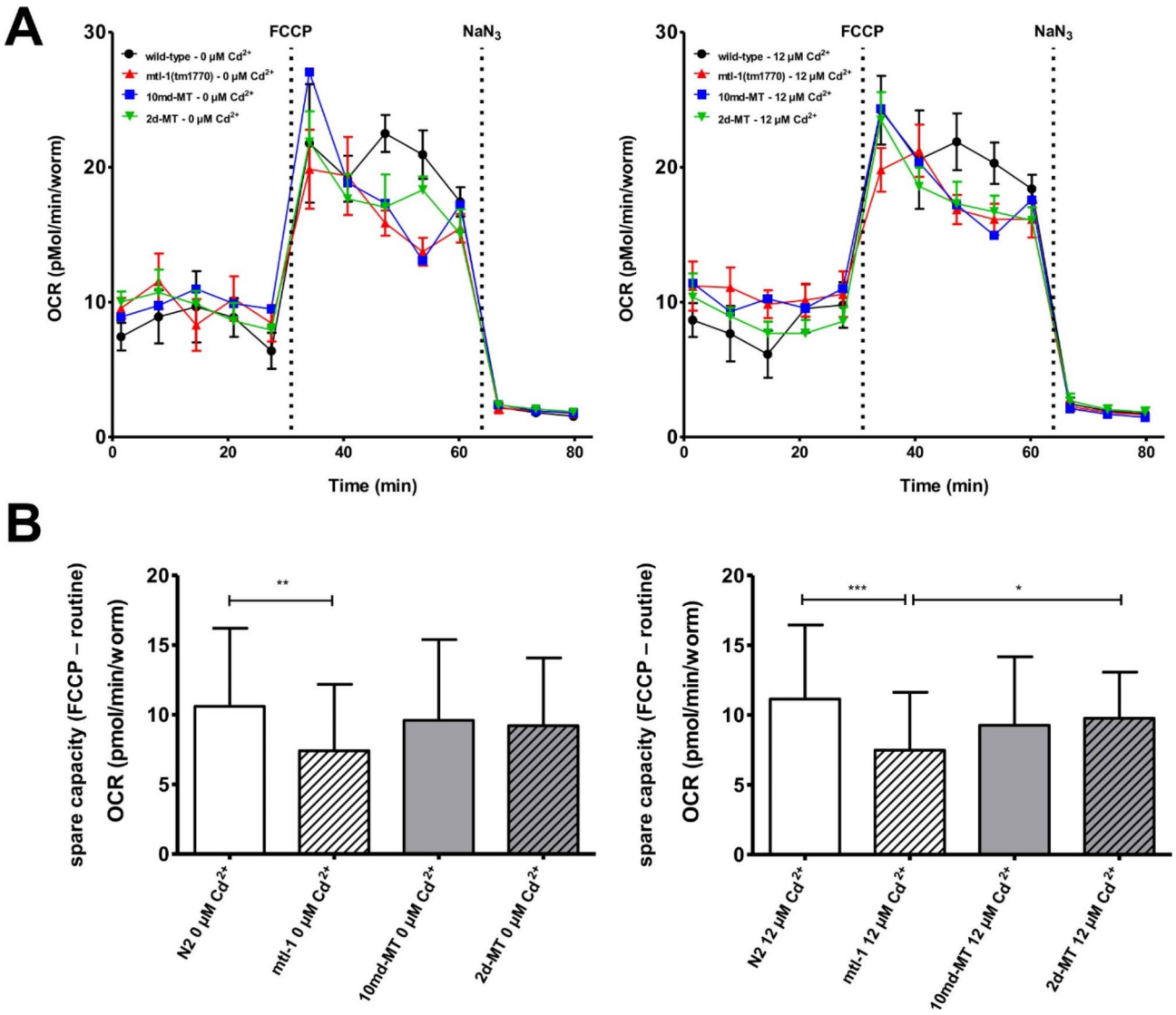

Fig. 5. Analysis of mitochondrial respiration suggests that MT expression rescues the mtl-1 knock-out but does not display any additional impact of Cd^{2+} to mitochondrial respiration in the nematode model. The top diagrams (**A**) display the original oxygen consumption rate (OCR), without any (left) and with 12 µM Cd^{2+} concentration (right) in the medium during the measurement. Calculated spare capacities are presented in the column diagram below (**B**). Statistical analysis involved 3 individual experiments for each strain, each referenced to N2, with three wells per strain in each experiment and approximately 20 worms per well. Error bars indicate the standard deviation at 95% confidence. Exact worm numbers were determined after the experiment. Significance is marked by asterisks.

its defense against Cd^{2+} toxicity[59], and thus relies on both MT-mediated and PCS-mediated pathways[85] to deal with Cd^{2+} and other metal ions[65]. Therefore, further experiments with an *mtl-1*/*mtl-2* double knock-out and with an *mtl-1*/*mtl-2*/*pcs-1* triple knock-out would be required to better understand the observed differences in the rescue effects of the two knock-in strains.

A

differences	size and diameter / nematode mass		% hatching worms at 0 µM Cd		% egg-laying mortality		viable offspring under Cd exposure		spare capacity (OCR) under Cd exposure	
reference strain	*wild type*	*mtl-1 (tm1770)*	*wild type*	*mtl-1 (tm1770)*	*wild type*	*mtl-1 (tm1770)*	*wild type*	*mtl-1 (tm1770)*	*wild type*	*mtl-1 (tm1770)*
10md-MT										
2d-MT										

not significant — *significant*

close to significance

B

rescue effect	size and diameter / nematode mass	% hatching worms at 0 µM Cd	% egg-laying mortality	viable offspring under Cd exposure	spare capacity (OCR) under Cd exposure
10md-MT	~	++	++	++	~
2d-MT	+	-	++	+	+

Fig. 6. Observed rescue effects in *C. elegans* MT knock-in strains. MT knock-in strains (*10md-MT* and *2d-MT*) referred to the *N2* wild-type or the MT-deficient *mtl-1* strain under control (no Cd^{2+} exposure) or Cd^{2+} exposure conditions. (**A**) Colors denote that observed effects are either not significant (grey) ($p > 0.05$ at 95% confidence), close to significance indicating a biological trend (light green) ($p > 0.07$), or significant (dark green) ($p < 0.05$ at 95% confidence). (**B**) Data of panel A is reduced to indicate the observed rescues effect of the two MT strains, compared to both reference strains (*N2*, *mtl-1*): '-' no rescue effect, '~' partial rescue effect, '+' rescue effect, '++' outperformance.

Data availability

Data is provided within the manuscript or supplementary information files. Full datasets generated and/or analyzed during the current study are available from the corresponding author upon reasonable request.

Received: 23 April 2024; Accepted: 11 October 2024
Published online: 26 October 2024

References

1. Chabicovsky, M., Klepal, W., Dallinger, R., Mechanisms of cadmium toxicity in terrestrial pulmonates: Programmed cell death and metallothionein overload. *Environ. Toxicol. Chem.* **23**, 648 (2004).
2. Martelli, A., Rousselet, E., Dycke, C., Bouron, A. & Moulis, J. M. Cadmium toxicity in animal cells by interference with essential metals. *Biochimie*. **88**, 1807–1814 (2006).
3. Swain, S. C., Keusekotten, K., Baumeister, R. & Stürzenbaum, S. R. *C. elegans* metallothioneins: New insights into the phenotypic effects of cadmium toxicosis. *J. Mol. Biol.* **341**, 951–959 (2004).
4. Choong, G., Liu, Y. & Templeton, D. M. Interplay of calcium and cadmium in mediating cadmium toxicity. *Chemico-Biol. Interact.* **211**, 54–65 (2014).
5. Soodvilai, S., Nantavishit, J., Muanprasat, C. & Chatsudthipong, V. Renal organic cation transporters mediated cadmium-induced nephrotoxicity. *Toxicol. Lett.* **204**, 38–42 (2011).
6. Satarug, S., Vesey, D. A. & Gobe, G. C. Cadmium-induced proteinuria: Mechanistic insights from dose–effect analyses. *Int. J. Mol. Sci.* **24**, 1893 (2023).
7. Fujiwara, Y. et al. Cadmium induces iron deficiency anemia through the suppression of iron transport in the duodenum. *Toxicol. Lett.* **332**, 130–139 (2020).
8. Klaassen, C. D., Liu, J. & Choudhuri, S. Metallothionein: An intracellular protein to protect against cadmium toxicity. *Annu. Rev. Pharmacol. Toxicol.* **39**, 267–294 (1999).
9. Kaegi, J. H. R. & Schaeffer, A. Biochemistry of metallothionein. *Biochemistry*. **27**, 8509–8515 (1988).
10. Romero-Isart, N. & Vašák, M. Advances in the structure and chemistry of metallothioneins. *J. Inorg. Biochem.* **88**, 388–396 (2002).
11. Vašák, M. Advances in metallothionein structure and functions. *J. Trace Elem. Med Biol.* **19**, 13–17 (2005).
12. Capdevila, M. & Atrian, S. Metallothionein protein evolution: A miniassay. *J. Biol. Inorg. Chem.* **16**, 977–989 (2011).

13. Blindauer, C. A. & Leszczyszyn, O. I. Metallothioneins: Unparalleled diversity in structures and functions for metal ion homeostasis and more. *Nat. Prod. Rep.* **27**, 720 (2010).
14. Krężel, A. & Maret, W. The functions of metamorphic metallothioneins in zinc and copper metabolism. *Int. J. Mol. Sci.* **18**, 1237 (2017).
15. Berger, B., Hunziker, P. E., Hauer, C. R., Birchler, N. & Dallinger, R. Mass spectrometry and amino acid sequencing of two cadmium-binding metallothionein isoforms from the terrestrial gastropod *Arianta arbustorum*. *Biochem. J.* **311**, 951–957 (1995).
16. Ziller, A. & Fraissinet-Tachet, L. Metallothionein diversity and distribution in the tree of life: A multifunctional protein. *Metallomics*. **10**, 1549–1559 (2018).
17. Zangger, K., ÖZ, G., Armitage, I. M. & Otvos, J. D. Three-dimensional solution structure of mouse [Cd7]-metallothionein-l by homonuclear and heteronuclear NMR spectroscopy. *Protein Sci.* **8**, 2630–2638 (2008).
18. Riek, R. et al. NMR structure of the sea urchin (*Strongylocentrotus purpuratus*) metallothionein MTA. *J. Mol. Biol.* **291**, 417–428 (1999).
19. Baumann, C. et al. Structural adaptation of a protein to increased metal stress: NMR structure of a Marine snail metallothionein with an additional domain. *Angew. Chem. Int. Ed.* **56**, 4617–4622 (2017).
20. Krezel, A. & Maret, W. Dual nanomolar and picomolar Zn(II) binding properties of metallothionein. *J. Am. Chem. Soc.* **129**, 10911–10921 (2007).
21. Suzuki, K. T., Someya, A., Komada, Y. & Ogra, Y. Roles of metallothionein in copper homeostasis: Responses to Cu-deficient diets in mice. *J. Inorg. Biochem.* **88**, 173–182 (2002).
22. Klaassen, C. D., Liu, J. & Diwan, B. A. Metallothionein protection of cadmium toxicity. *Toxicol. Appl. Pharmcol.* **238**, 215–220 (2009).
23. Min, K. S., Terano, Y., Onosaka, S. & Tanaka, K. Induction of hepatic metallothionein by nonmetallic compounds associated with acute-phase response in inflammation. *Toxicol. Appl. Pharmcol.* **111**, 152–162 (1991).
24. Cai, L., Satoh, M., Tohyama, C. & Cherian, M. G. Metallothionein in radiation exposure: Its induction and protective role. *Toxicology*. **132**, 85–98 (1999).
25. Ling, X. B. et al. Mammalian metallothionein-2A and oxidative stress. *Int. J. Mol. Sci.* **17**, 1483 (2016).
26. Cui, Y. et al. ECRG2, a novel candidate of tumor suppressor gene in the esophageal carcinoma, interacts directly with metallothionein 2A and links to apoptosis. *Biochem. Biophys. Res. Commun.* **302**, 904–915 (2003).
27. Giacconi, R. et al. Novel – 209A/G MT2A polymorphism in old patients with type 2 diabetes and atherosclerosis: Relationship with inflammation (IL-6) and zinc. *Biogerontology* 6, 407–413 (2005).
28. Qu, W., Pi, J. & Waalkes, M. P. Metallothionein blocks oxidative DNA damage in vitro. *Arch. Toxicol.* **87**, 311–321 (2013).
29. Palmiter R. D. The elusive function of metallothioneins. *Proc. Natl. Acad. Sci.* **95**, 8428–8430 (1998).
30. Isani, G. & Carpenè, E. Metallothioneins, Unconventional proteins from unconventional animals: A long journey from nematodes to mammals. *Biomolecules*. **4**, 435–457 (2014).
31. Haq, F. Signaling events for metallothionein induction. *Mutat. Research/Fundamental Mol. Mech. Mutagen.* **533**, 211–226 (2003).
32. West, A. K., Stallings, R., Hildebrand, C. E., Chiu, R., Karin, M. & Richards, R. I. Human metallothionein genes: Structure of the functional locus at 16q13. *Genomics*. **8**, 513–518 (1990).
33. Koizumi, S., Suzuki, K., Ogra, Y., Yamada, H. & Otsuka, F. Transcriptional activity and regulatory protein binding of metal-responsive elements of the human metallothionein-IIA gene. *Eur. J. Biochem.* **259**, 635–642 (2001).
34. Stuart, G. W., Searle, P. F. & Palmiter, R. D. Identification of multiple metal regulatory elements in mouse metallothionein-I promoter by assaying synthetic sequences. *Nature*. **317**, 828–831 (1985).
35. Lichtlen, P. & Schaffner, W. Putting its fingers on stressful situations: The heavy metal-regulatory transcription factor MTF-1. *BioEssays*. **23**, 1010–1017 (2001).
36. Günther, V., Lindert, U. & Schaffner, W. The taste of heavy metals: Gene regulation by MTF-1. *Biochim. et Biophys. Acta (BBA) - Mol. Cell. Res.* **1823**, 1416–1425 (2012).
37. Giedroc, D. P., Chen, X. & Apuy, J. L. Metal response element (MRE)-Binding transcription Factor-1 (MTF-1): Structure, function, and Regulation. *Antioxid. Redox. Signal.* **3**, 577–596 (2001).
38. Dalton, T. P., Solis, W. A., Nebert, D. W. & Carvan, M. J. III Characterization of the MTF-1 transcription factor from zebrafish and trout cells. *Comp. Biochem. Physiol. B: Biochem. Mol. Biol.* **126**, 325–335 (2000).
39. Andrews, G. K. Regulation of metallothionein gene expression by oxidative stress and metal ions. *Biochem. Pharmacol.* **59**, 95–104 (2000).
40. Stitt, M. S. et al. Nitric oxide-induced nuclear translocation of the metal responsive transcription factor, MTF-1 is mediated by zinc release from metallothionein. *Vascul. Pharmacol.* **44**, 149–155 (2006).
41. Murphy, B. J. et al. Activation of metallothionein gene expression by hypoxia involves metal response elements and metal transcription factor-1. *Cancer Res.* **59**, 1315–1322 (1999).
42. Egli, D. et al. A family knockout of all four *Drosophila metallothioneins* reveals a central role in copper homeostasis and detoxification. *Mol. Cell. Biol.* **26**, 2286–2296 (2006).
43. Dallinger, R. et al. Metallomics reveals a persisting impact of cadmium on the evolution of metal-selective snail metallothioneins. *Metallomics*. **12**, 702–720 (2020).
44. Palacios, Ò. et al. Shaping mechanisms of metal specificity in a family of metazoan metallothioneins: Evolutionary differentiation of mollusc metallothioneins. *BMC Biol.* **9**, 4 (2011).
45. Palacios, Ò. et al. Analysis of metal-binding features of the wild type and two domain-truncated mutant variants of *Littorina littorea* metallothionein reveals its Cd-specific character. *Int. J. Mol. Sci.* **18**, 1452 (2017).
46. Schmielau, L. et al. Differential response to cadmium exposure by expression of a two and a three-domain metallothionein isoform in the land winkle *Pomatias elegans*: Valuating the marine heritage of a land snail. *Sci. Total Environ.* **648**, 561–571 (2019).
47. Dallinger, R., Berger, B., Hunziker, P. & Kgi, J. H. R. Metallothionein in snail Cd and Cu metabolism. *Nature*. **388**, 237–238 (1997).
48. Palacios, Ò. et al. Cognate and noncognate metal ion coordination in metal-specific metallothioneins: The Helix pomatia system as a model. *J. Biol. Inorg. Chem.* **19**, 923–935 (2014).
49. Dallinger, R. Metals and metallothionein evolution in snails: A contribution to the concept of metal-specific functionality from an animal model group. *Biomet. Int. J. role Metal Ions Biol. Biochem. Med.*https://doi.org/10.1007/s10534-024-00584-3 (2024).
50. Höckner, M. et al. Physiological relevance and contribution to metal balance of specific and non-specific metallothionein isoforms in the garden snail, *Cantareus aspersus*. *BioMetals*. **24**, 1079–1092 (2011).
51. Egg, M., Höckner, M., Brandstätter, A., Schuler, D. & Dallinger, R. Structural and bioinformatic analysis of the roman snail Cd-metallothionein gene uncovers molecular adaptation towards plasticity in coping with multifarious environmental stress. *Mol. Ecol.* **18**, 2426–2443 (2009).
52. Benito, D., Niederwanger, M., Izagirre, U., Dallinger, R. & Soto, M. Successive onset of Molecular, Cellular and tissue-specific responses in Midgut Gland of *Littorina littorea* exposed to sub-lethal cadmium concentrations. *Int. J. Mol. Sci.* **18**, 1815 (2017).
53. Dvorak, M. et al. Metal binding functions of metallothioneins in the slug *Arion vulgaris* differ from metal-specific isoforms of terrestrial snails. *Metallomics*. **10**, 1638–1654 (2018).
54. Pedrini-Martha, V., Köll, S., Dvorak, M., & Dallinger, R. Cadmium Uptake, MT gene activation and structure of large-sized multi-domain metallothioneins in the terrestrial door snail *Alinda biplicata* (Gastropoda, Clausiliidae). *Int. J. Mol. Sci.* **21**, 1631 (2020).
55. Brenner, S. The genetics of *Caenorhabditis elegans*. *Genetics*. **77**, 71–94 (1974).
56. Nance, J. & Frøkjær-Jensen, C. The *Caenorhabditis elegans* Transgenic Toolbox. *Genetics*. **212**, 959–990 (2019).

57. Goussen, B. et al. R. Energy-based modelling to assess effects of chemicals on *Caenorhabditis elegans*: A case study on uranium. *Chemosphere*. **120**, 507–514 (2015).
58. Byerly, L., Cassada, R. C. & Russell, R. L. The life cycle of the nematode *Caenorhabditis elegans*. *Dev. Biol.* **51**, 23–33 (1976).
59. Hall, J., Haas, K. L. & Freedman, J. H. Role of MTL-1, MTL-2, and CDR-1 in mediating cadmium sensitivity in *Caenorhabditis elegans*. *Toxicol. Sci.* **128**, 418–426 (2012).
60. Essig, Y. J. et al. Juggling cadmium detoxification and zinc homeostasis: A division of labour between the two *C. elegans* metallothioneins. *Chemosphere*. **350**, 141021 (2024).
61. Imagawa, M. et al. Characterization of metallothionein cDNAs induced by cadmium in the nematode *Caenorhabditis elegans*. *Biochem. J.* **268**, 237–240 (1990).
62. Freedman, J. H., Slice, L. W., Dixon, D., Fire, A. & Rubin, C. S. The novel metallothionein genes of *Caenorhabditis elegans*. Structural organization and inducible, cell-specific expression. *J. Biol. Chem.* **268**, 2554–2564 (1993).
63. Moilanen, L. H., Fukushige, T. & Freedman, J. H. Regulation of metallothionein gene transcription. *J. Biol. Chem.* **274**, 29655–29665 (1999).
64. Hughes, S. & Stürzenbaum, S. R. Single and double metallothionein knockout in the nematode *C. elegans* reveals cadmium dependent and independent toxic effects on life history traits. *Environ. Pollut.* **145**, 395–400 (2007).
65. Zeitoun-Ghandour, S. et al. The two *Caenorhabditis elegans* metallothioneins (CeMT-1 and CeMT-2) discriminate between essential zinc and toxic cadmium. *FEBS J.* **277**, 2531–2542 (2010).
66. Dong, J., Song, M. O. & Freedman, J. H. Identification and characterization of a family of *Caenorhabditis elegans* genes that is homologous to the cadmium-responsive gene cdr-1. *Biochim. et Biophys. Acta (BBA) - Gene Struct. Expression*. **1727**, 16–26 (2005).
67. Vatamaniuk, O. K., Bucher, E. A., Sundaram, M. V. & Rea, P. A. CeHMT-1, a putative phytochelatin transporter, is required for cadmium tolerance in *Caenorhabditis elegans*. *J. Biol. Chem.* **280**, 23684–23690 (2005).
68. Andrássy, I. Die rauminhalst and gewichtsbestimmung Der fadenwurmer (Nematoden). *Acta Zool. Academi Sci.* **2**, 1–15 (1956).
69. Koopman, M. et al. A screening-based platform for the assessment of cellular respiration in *Caenorhabditis elegans*. *Nat. Protoc.* **11**, 1798–1816 (2016).
70. Preez, G. et al. Oxygen consumption rate of *Caenorhabditis elegans* as a high-throughput endpoint of toxicity testing using the seahorse XFe96 Extracellular Flux Analyzer. *Sci.Rep.* **10**, 4239 (2020).
71. Luz, A. L., Smith, L. L., Rooney, J. P. & Meyer, J. N. Seahorse Xfe 24 extracellular flux analyzer-based analysis of cellular respiration in *Caenorhabditis elegans*. *Curr. Protocols Toxicol.* **66**, (2015). 25.7.1–25.7.15.
72. Luz, A. L. et al. Mitochondrial morphology and fundamental parameters of the mitochondrial respiratory chain are altered in *Caenorhabditis elegans* strains deficient in mitochondrial dynamics and Homeostasis processes. *PloS One*. **10**, e0130940 (2015).
73. Dilberger, B. et al. Mitochondrial oxidative stress impairs energy metabolism and reduces stress resistance and longevity of *C. elegans*. *Oxidative medicine and cellular longevity* **6840540** (2019). (2019).
74. Mello, D. F. et al. Rotenone modulates *Caenorhabditis elegans* immunometabolism and pathogen susceptibility. *Front. Immunol.* **13**, 840272 (2022).
75. So, S., Miyahara, K. & Ohshima, Y. Control of body size in *C. elegans* dependent on food and insulin/IGF-1 signal. *Genes Cells: Devoted Mol. Cell. Mech.* **16**, 639–651 (2011).
76. Bofill, R. et al. *Caenorhabditis elegans* metallothionein isoform specificity – metal binding abilities and the role of histidine in CeMT1 and CeMT2. *FEBS J.* **276**, 7040–7056 (2009).
77. Wang, S., Chu, Z., Zhang, K. & Miao, G. Cadmium-induced serotonergic neuron and reproduction damages conferred lethality in the nematode *Caenorhabditis elegans*. *Chemosphere*. **213**, 11–18 (2018).
78. Athar, F. & Templeman, N. M. *C. elegans* as a model organism to study female reproductive health. *Comp. Biochem. Physiol. A Mol. Integr. Physiol.* **266**, 111152 (2022).
79. Swain, S. et al. Linking toxicant physiological mode of action with induced gene expression changes in *Caenorhabditis elegans*. *BMC Syst. Biol.* **4**, 32 (2010).
80. Höckner, M., Dallinger, R. & Stürzenbaum, S. R. Nematode and snail metallothioneins. *J. Biol. Inorg. Chem.* **16**, 1057–1065 (2011).
81. Uppaluri, S. & Brangwynne, C. A size threshold governs *Caenorhabditis elegans* developmental progression. *Proc. Biol. Sci.* **282**, 20151283 (2015).
82. Calap-Quintana, P., González-Fernández, J., Sebastiá-Ortega, N., Llorens, J. & Moltó, M. *Drosophila melanogaster* models of metal-related human diseases and metal toxicity. *Int. J. Mol. Sci.* **18**, 1456 (2017).
83. Lee, W. K. & Thévenod, F. Cell organelles as targets of mammalian cadmium toxicity. *Arch. Toxicol.* **94**, 1017–1049 (2020).
84. Branca, J. J. V. et al. Cadmium-induced cytotoxicity: Effects on mitochondrial electron transport chain. *Front. Cell. Dev. Biology* **8**, (2020).
85. Clemens, S., Schroeder, J. I. & Degenkolb, T. *Caenorhabditis elegans* expresses a functional phytochelatin synthase. *Eur. J. Biochem.* **268**, 3640–3643 (2001).

Acknowledgements

The authors are very thankful for the technical assistance by Samantha Hughes, Konstanze Simbriger, Paula Schmidt, Simon Köll, and Tiziano Paravicini. The work presented in this manuscript was funded in whole by the Austrian Science Fund (FWF), project P 33973-B [DOI: https://doi.org/10.55776/P33973] to Reinhard Dallinger and Veronika Pedrini-Martha. For open access purposes, the author has applied for a CC BY public copyright license to any author accepted manuscript version arising from this submission.

Author contributions

Eva Albertini conceived and created the *10md-MT* knock-in strain based on the *mtl-1* strain and planned the genotyping. Michael Niederwanger performed AAS experiments and qRT-PCR. Andreas Andric performed all nematode related experiments, including egg-laying and Seahorse Flux Analysis. Stephen Stürzenbaum provided the backcrossed *mtl-1* strain used in this study. Alexander Weiss, Veronika Pedrini-Martha, Reinhard Dallinger, and Pidder Jansen-Dürr conceived and supervised the experiments. Andreas Andric, Alexander Weiss, Veronika Pedrini-Martha and Reinhard Dallinger performed data analysis and conceived the manuscript. Alexander Weiss, Veronika Pedrini-Martha and Reinhard Dallinger contributed the financial support. Alexander Weiss, Pidder Jansen-Dürr, Stephen Stürzenbaum, Veronika Pedrini-Martha and Reinhard Dallinger conducted the review and refinement of the manuscript.

Declarations

Competing interests

The authors declare no competing interests.

Additional information

Supplementary Information The online version contains supplementary material available at https://doi.org/10.1038/s41598-024-76268-2.

Correspondence and requests for materials should be addressed to R.D., V.P.-M. or A.K.H.W.

Reprints and permissions information is available at www.nature.com/reprints.

Publisher's note Springer Nature remains neutral with regard to jurisdictional claims in published maps and institutional affiliations.